

## A Calibration for Surface Analysis on Aluminium Alloys by RF-Glow-Discharge Optical Emission Spectrometry

J.M. Long<sup>1</sup>, P.J.K. Paterson<sup>2</sup>, and A.E. Hughes<sup>3</sup>

<sup>1</sup>*School of Engineering and Technology, Deakin University, Geelong, Victoria*

<sup>2</sup>*Department of Applied Physics, RMIT University, Melbourne, Victoria*

<sup>3</sup>*CSIRO Manufacturing and Infrastructure Technology, Clayton, Victoria*

*e-mail of corresponding author: jlong@deakin.edu.au*

### Introduction

Characterisation of surface modification in solids has become an increasingly important field in materials science and engineering [1]. In the aerospace industry aluminium alloys are used in a variety of components where the nature of the surface is important in determining performance. In particular, the surface-related phenomenon of corrosion can lead to shortening of component lifetime, and potentially catastrophic failure. To protect against corrosion, the native oxide is replaced by a conversion coating which has better corrosion resistance. Corrosion products, native oxides and conversion coatings are all insulating layers which charge electrically under many forms of surface analysis. This is not the case for Radiofrequency glow-discharge optical emission spectroscopy (RF-GD-OES). It has the great advantage of being able to depth profile through multiple layers, both conducting and insulating, without need for charge compensation or correction [2].

Traditional direct-current DC-GD-OES allows depth profiling on electrically conductive surfaces only. Our previous studies of thin oxide layers on aluminium by DC-GD-OES have produced some limited results. For instance, we have been able to obtain quantitative elemental depth profiles of very thin oxide layers on aluminium castings [3]. Some depth profiles were obtained on the aerospace alloy AA7475, but in this case oxygen was not measured by GD-OES. Depth profiling for oxygen on this material by other methods yielded qualitative results [4]. From our further work on other aluminium alloys and conversion coatings, DC-GD-OES has proven difficult to unsuitable for the analysis of these insulating layers. Fully quantitative depth profiles of oxidised aluminium by RF-GD-OES has been scarce in the literature [5]. Qualitative results are more common [6].

In this study, an RF calibration was produced by sputtering and collecting elemental emission intensities from a range of certified aluminium standards. A sample of AA7475-7651 (a tempered ALCOA product) was sputter depth profiled with the sputtered depths calibrated using relative sputter rates obtained from the sputter yields of each major element with corrections for composition and discharge conditions. We employed the multi-matrix calibration method as developed by Bengston, Weiss, and colleagues [7,8]. For a given element  $E$  being measured by means of atomic emission line  $\lambda$ , the detected intensity in volts of the emission line is given by

$$I_{\lambda E} = R_E q_m c_{EM} + I_0$$

In this equation,  $c_{EM}$  is the concentration (wt%) of element  $E$  in bulk material  $M$ .  $R_E$  is the emission yield of element  $E$ ,  $q_m$  is the sputter rate of the sample in micro-grams per second, and  $I_0$  is background noise. We assume that there are no inter-element interferences or corrections. By calibration, all the emission yields, correction factors, and the background are either known or measured. It is then possible to determine the concentrations of elements in

an unknown sample as a function of time. In a depth profile, the unknown sputter rate at some instant is determined by first normalising the sum of all the concentrations of all the elements in the sample to 100%. Then the sputter rate, followed by the sample density, as functions of time are calculated, from which it is possible to determine the sputtered volume as a function of time. The sampling area is equal to the anode area, and it is then possible to determine quantitative elemental concentrations versus depth in microns.

### Experimental

Table 1 shows the standards used for this calibration, and Table 2 shows the selected emission lines for the analysis. We employed a Leco GDS-850A GD-OES spectrometer for the analysis [9]. It was fitted with a 4-mm anode. The RF-lamp was operated in power-voltage mode, where the RF power was fixed at 14 watts. A variable argon pressure held the lamp voltage fixed at 700 volts. The resulting plasma current was 20 mA. Three burns were obtained from each standard. Once all the standards were measured, calibration curves for each element were plotted: weight percent multiplied by the standard's sputter rate versus the measured spectral line intensity in volts. The gradient of each calibration curve produces the emission yield for each element.

**Table 1: Standards used and certified elemental concentrations (wt%).**

Standard	Al	Cr	Cu	Fe	Mg	Mn	Ni	Si	Ti	Zn	O	N
SS1050-2	99.56	0.005	0.041	0.28	0.00	0.002	0.001	0.093	0.004	0.001		
SA1838-30	98.1	0.083	0.11	0.19	0.90	0.041	0.035	0.50	0.014	0.028		
SS2117-D	96.02	0.03	2.61	0.41	0.26	0.054	0.031	0.51	0.022	0.056		
SS7075-AR	89.18	0.23	1.64	0.24	2.63	0.085	0.004	0.17	0.041	5.78		
SS5182-DV	94.49	0.031	0.051	0.21	4.62	0.35	0.022	0.15	0.028	0.05		
SS5052-CA	96.57	0.26	0.062	0.20	2.57	0.058	0.053	0.12	0.15	0.081		
SS2024-U20	92.49	0.059	4.54	0.33	1.60	0.61	0.048	0.21	0.034	0.074		
LCI-8	0.008	0.062	0.550	90.64	0.092	1.101	1.46	1.47	0.021			
BS825B	0.10	20.06	1.64	35.10	0.002	0.49	38.70	0.0004	0.740		0.001	0.007
CC-650	36.50				0.0195				23.20		32.40	4.90
Coronite		4.0		48.90		0.10			25.0			6.9

**Table 2: Emission lines employed for the analysis.**

Element Analyzed	Spectral Line (nm)	Element Analyzed	Spectral Line (nm)	Element Analyzed	Spectral Line (nm)
Al	396.152	Mg	383.829	Ti	337.279
Cr	425.443	Mn	403.449	Zn	330.258
Cu	327.396	Ni	341.447	O	130.217
Fe	371.994	Si	288.158	N	174.272
C	165.701				

### Results and Discussion

Table 3 shows the calibration results for aluminium, and Table 4 shows the resulting calibration curve parameters for all the elements. Except for magnesium, all the calibration curves were linear. A non-linear calibration curve in GD-OES usually occurs when the concentration range for the particular element is very large. The result found for magnesium is under further investigation. The goodness-of-fit for oxygen and nitrogen were both zero

because these two elements had only two points on the calibration curve. This is because suitable standards for oxygen and nitrogen are scarce.

**Table 3: Aluminium calibration curve.**

Standard	Al line intensity (volts)	Calculated wt%	Certified wt%	Percent difference	Standard deviation
SS1050-2	1.978	99.10	99.56	-0.46	0.02
SA1838-30	1.751	97.79	98.10	-0.31	0.01
SS2117-D	2.022	95.91	96.02	-0.11	0.1
SS7075-AR	1.955	90.09	89.18	1.03	0.002
SS5182-DV	1.695	94.17	94.49	-0.34	0.006
SS5052-CA	1.707	96.58	96.57	0.011	0.01
SS2024-U20	2.053	92.55	92.49	0.063	0.1
CC-650	0.3832	36.60	36.50	0.26	0.006

**Table 4: Calibration results for all elements.**

Element analyzed	y-intercept	Linear component	Second-order component	Goodness of fit factor
Al	$1.394 \times 10^{-2}$	$4.956 \times 10^{-2}$	0	0.40
Cr	$-8.039 \times 10^{-5}$	$2.417 \times 10^{-2}$	0	0.025
Cu	$1.087 \times 10^{-6}$	$3.009 \times 10^{-2}$	0	0.093
Fe	$-2.784 \times 10^{-5}$	$2.322 \times 10^{-2}$	0	0.033
Mg	$-4.748 \times 10^{-5}$	$4.529 \times 10^{-2}$	0.1318	0.15
Mn	$-4.361 \times 10^{-5}$	$2.013 \times 10^{-2}$	0	0.023
Ni	$-4.623 \times 10^{-5}$	$1.193 \times 10^{-2}$	0	0.0035
Si	$-8.039 \times 10^{-5}$	$2.417 \times 10^{-2}$	0	0.025
Ti	0.000	$3.328 \times 10^{-2}$	0	0.12
Zn	$-2.178 \times 10^{-4}$	0.1959	0	0.0084
O	$-7.669 \times 10^{-3}$	0.3290	0	0.0
N	$2.509 \times 10^{-3}$	0.1183	0	0.0
C	$1.748 \times 10^{-4}$	$2.647 \times 10^{-3}$	0	0.23

With the calibration complete, a tempered form of aluminium alloy 7475, in its naturally oxidised state, was measured for its elemental depth profile. For selected elements, the resulting, fully-quantitative depth profile is shown in Figure 1. The existence of multiple layers is evident. A carbon-rich layer was detected in the first 100-200 nm (a common impurity found on the surface of metal samples). Some surface segregation of silicon was also detected here. This was followed by a mixture of aluminium and magnesium oxides for the next 400 nm. Following this is a mainly aluminium oxide layer over 500-800 nm. High nitrogen in the surface is also visible and begins to disappear at this point. Another magnesium-rich region exists over 800 nm to 1.5 microns. In this layer the oxygen content decreases smoothly. Evidence of oxygen in the surface persists to a depth of three microns. These results are consistent with our previous studies of similar alloys [4], which showed on the surface significant magnesium enrichment, a complex structure of magnesium and aluminium oxides, and perhaps some spinel. Unlike our previous GD-OES work, this new investigation clearly shows the depth and concentration of the oxide layers.

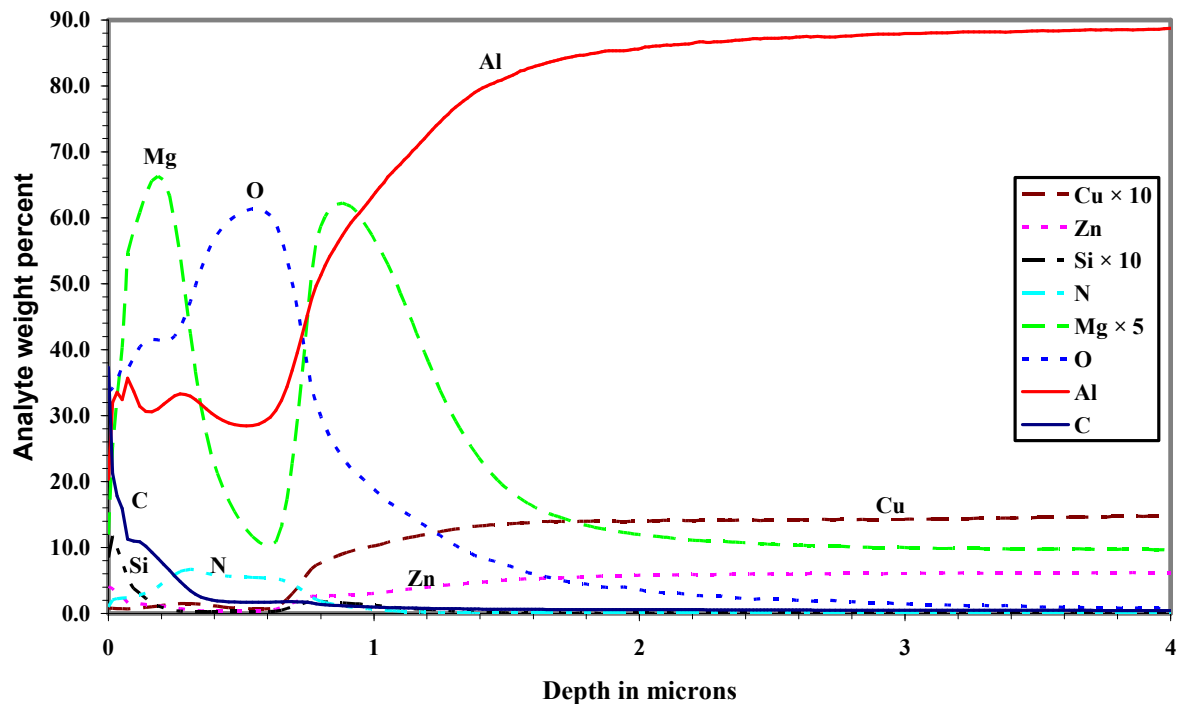


Figure 1: Quantitative depth profile for tempered aluminium alloy 7475.

### Conclusion

A calibration for the technique of RF-GD-OES is presented for use on oxidised aluminium alloys. RF-GD-OES has proven to be more suitable than its DC counterpart when a significant insulating oxide layer is present. The application of this new method on the native oxide of a tempered 7475 aluminium alloy shows significant magnesium enrichment and a complex multi-layer structure of aluminium and magnesium oxides in the first two microns of the metal. The method shows great promise for the rapid surface analysis of oxidised and anodised aluminium, and related conversion coatings.

### References

- [1] J.B. Hudson, *Surface Science: an Introduction* (Wiley, 1998)
- [2] K. Shimizu, H. Habazaki, P. Skeldon, and G.E. Thompson, *Spectrochimica Acta* **B58**, 1573-1583 (2003)
- [3] J.M. Long, *Proceedings of the 27th Annual A&NZIP Condensed Matter and Materials Meeting*, editors J. Cashion, T. Finlayson, D. Paganin, A. Smith, and G. Troup (Australian Institute of Physics, 2003), <http://www.aip.org.au/wagga2003/Hubpage.pdf>
- [4] S.K. Toh, D.G. McCulloch, J. DuPlessis, P.J.K. Paterson, A.E. Hughes, D. Jamieson, B. Rout, J.M. Long, and A. Stonham, *Surface Review and Letters*, **10**, 365-371 (2003)
- [5] J.T.B. Gundersen, A. Aytac, S. Ono, J.H. Nordlien, and K. Nisancioglu, *Corrosion Science* **46**, 265-283 (2004)
- [6] K. Shimizu, G.M. Brown, H. Habazaki, K. Kobayashi, P. Skeldon, G.E. Thompson, and G.C. Wood, *Surface and Interface Analysis* **27**, 24-28 (1999)
- [7] A. Bengston, *Spectrochimica Acta* **B49**, 411-429 (1994)
- [8] Z. Weiss, in *Glow Discharge Optical Emission Spectrometry*, editors R. Payling, D.G. Jones and A. Bengston (Wiley, 1997)
- [9] J.M. Long, *Proceedings of Engineering Materials 2001*, editors E. Pereloma and K. Raviprasad, **i**, 87-92 (Institute of Materials Engineering Australasia, 2001)